Water Practice & Technology

IWA PUBLISHING

Water Practice & Technology Vol 17 No 6, 1305 doi: 10.2166/wpt.2022.060

Removal of sediment through hydro-suction revisited: An extensive review of the hydro-suctioning method, widely used for sediment removal from the water bodies

Akash Jaiswal [a,*], Z. Ahmad[b] and S. K. Mishra[a]

[a] WRDM, IIT Roorkee, Roorkee, Uttarakhand, India
[b] CED, IIT Roorkee, Roorkee, Uttarakhand, India
*Corresponding author. E-mail: akaskjaiswal@gmail.com

AJ, 0000-0001-9141-9322

ABSTRACT

Hydro-suctioning is used to remove the deposited sediment from water bodies. A suction pipe is placed on/above/below the sediment bed, and deposited sediment is removed using suction. The sediment movement during hydro-suction, flow pattern, temporal sediment concentration, and scour profile are reviewed extensively and summarized in this paper. It is seen that the sediment removal initiates due to lift forces and continues further due to a change in flow field that creates sediment resuspension. The sediment removal ceases if the suction inlet reaches a distance, i.e., critical suction inlet depth. Within this critical zone, when the hydro-suction initiates, sediment just below the suction pipe is first removed, leading to the maximum scour depth, i.e., below the sediment bed level. In this process, sediment from sides of the scour hole is hydrodynamically dragged towards the center, where it gets deposited, and a hump is formed at the center. At equilibrium, the sediment removal ceases. This paper discusses the equations predicting scour profile and critical inlet depth. It is seen that the research work dealing with the standardization of hydro-suction for fixation of suction pipe diameter, suction inlet depth, discharge, etc. is in quite a primitive stage and needs urgent attention.

Key words: flow pattern, hydro-suction, removal equations, scour profile, sediment movement, temporal sediment concentration

HIGHLIGHTS

- Sedimentation in water bodies.
- Sediment removal through hydro-suction.
- Flow pattern near the mouth of the suction pipe.
- Formation of scour profile due to hydro-suction.
- Temporal variation of sediment concentration in the suction pipe.

GRAPHICAL ABSTRACT

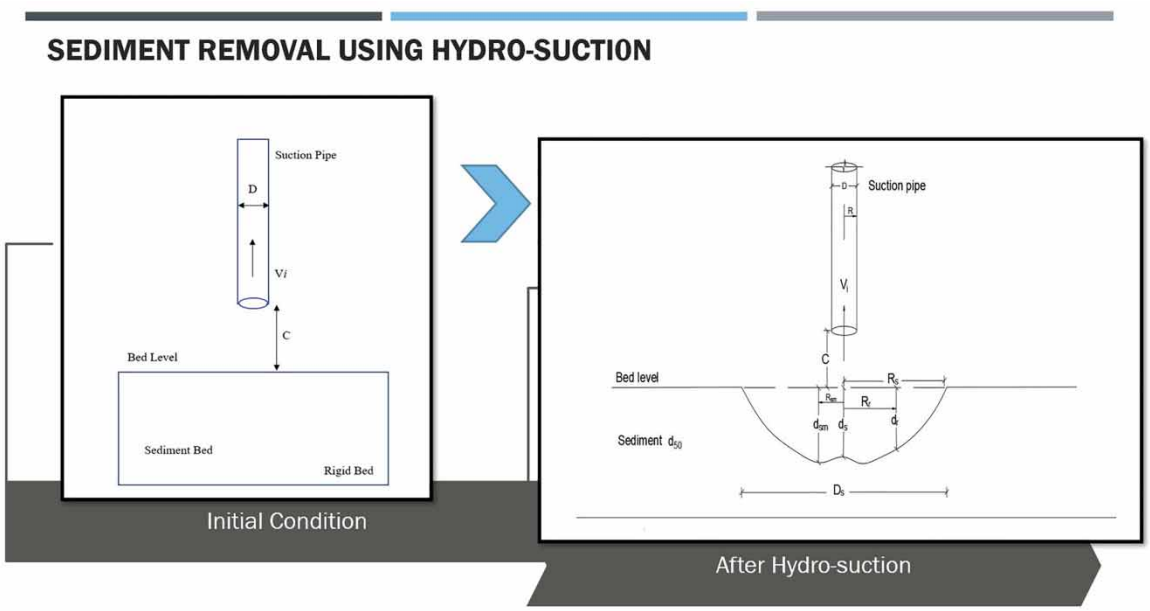

INTRODUCTION

Reservoir sedimentation generally results from natural and anthropogenic causes, as defined by Obialor *et al.* (2019). The morphology of a river changes through sediment deposition and scour. To apply engineering solutions, it is necessary to understand the principles of sediment movement (Zakaria *et al.* 2010). Sediment transportation depends on the size, density, volume, and shape of the particle and the strength of the flow (Azamathulla *et al.* 2013). Sedimentation poses a significant danger to the adequate life of the dam and, consequently, its purpose. It causes loss in the storage of dam, blocks the water inlet of irrigation and hydropower, damages the rotor blades of the hydropower turbine, causes a loss to surrounding ecology and ecosystem, damages the spillway gate or other vital structures, and even may damage the dam. Sedimentation can change river elevation for several kilometers downstream, promoting migration of river reach and causing a loss in channel capacity (Azamathulla 2014). A survey done over 238 dams in 19 states of India indicates that the national average reservoir capacity loss is about 15% of reservoir capacity with a maximum of 30%. The national average of observed sedimentation rate is 1.41% of reservoir capacity per year with a maximum of 3.8% (Patra *et al.* 2019). This data highlights the seriousness of the situation and signposts its adverse effects in the near future. Thus, there is a need for a strategic process to cope with the sedimentation in water bodies.

Hydro-suction is a process used to remove sediment deposited on the bed of rivers. A suction pipe is placed vertically below/on/above the sediment bed. During hydro-suction, bed materials are sheared to resuspension and then sucked in with the water flow generated by suction. With the initiation of hydro-suction, sediment removal starts, thus creating a scour hole below the suction inlet and continuing until the deepest scour hole is reached. Sediment gets dragged from the periphery and deposited near the center of scour hole, thus forming a hump at the center. The scour depth and radius change with suction pipe diameter, suction inlet depth, sediment size, and inlet discharge. Flow patterns, bed material movement in the vicinity of the suction inlet, sediment concentration in the suction pipe, and scour hole formation are points of concern for the hydro-suction removal. Knowing these, one would design the governing components of a hydro-suction system.

A definition sketch of hydro-suction is shown in Figure 1, in which V_i is inlet velocity, D is suction pipe diameter, C is suction inlet depth (the distance between the suction inlet and bed level), d_{50} is sediment median size, R_s is scour radius, D_s is scour diameter ($2R_s$), d_s is scour depth just below the suction pipe, R_{sm} is scour radius at maximum scour depth (d_{sm}), and d_r is scour depth at any scour radius R_r, as shown in Figure 1.

Brahme & Herbich (1986) was the pioneer of studying the hydraulic model to design hydro-suction for sediment removal. Rehbinder (1994) studied the applicability of hydro-suction for sediment removal, focusing on the initial movement of sediment. Following this, Hotchkiss & Huang (1995), Ullah *et al.* (2005), Su-Chin

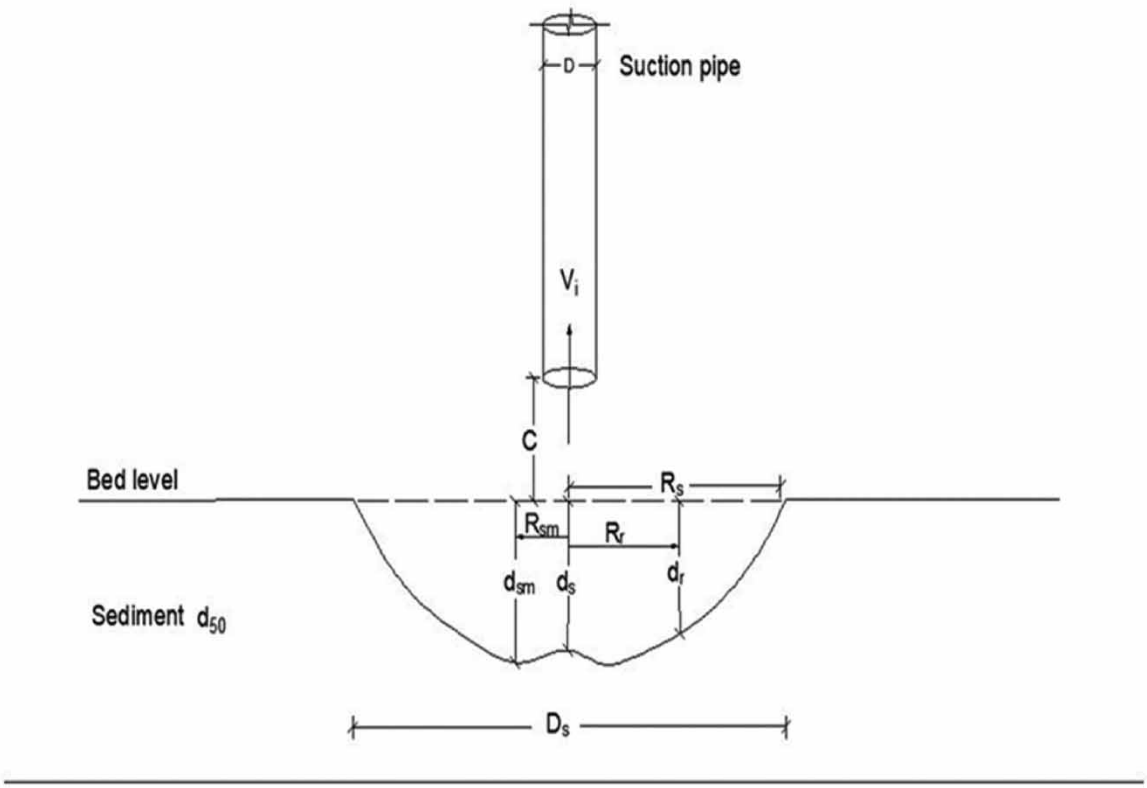

Figure 1 | Definition sketch of a hydro-suction (Ullah *et al.* 2005).

et al. (2010), Shrestha (2012), Zhou *et al.* (2013), Sadatomi *et al.* (2015), Ke *et al.* (2016), Asiaban *et al.* (2017), Pishgar *et al.* (2018), Elgamal & Fouli (2020) and Pu Yang *et al.* (2020) further stepped up the investigation to analyze all the factors involved in the hydro-suction. In literature, suction pipe diameters ranging from 0.002 m to 0.08 m and sediment sizes ranging from 0.005 to 4 mm were studied thoroughly for hydro-suction removal of sediment. Investigators used these sediment samples from different locations and took their median size through particle size analysis. Along with these, geometrical modifications of suction pipe, different shapes of pipe, and different types of sediments were studied by investigators such as Brahme & Herbich (1986), Asiaban *et al.* (2017), and Pishgar *et al.* (2018). Using the siphon method, Tong *et al.* (2010) investigated the dewatering behavior of horizontally installed drainage plates. Zulkefli *et al.* (2019) reviewed the usage of siphon technique for sediment removal. Along with the experimental investigations, C.F.D. Tools can also predict the sediments scour. C.F.D. Tools can predict sediment motion in any fluid, though all sediment motion must occur within one fluid (Tajari *et al.* 2020).

Analytical and experimental analyses were performed in the past to understand hydro-suction. Several mathematical expressions were also derived governing the removal of sediments and geometry of scour hole. The review in this paper will help to understand the hydro-suction removal of sediment, flow pattern and scour formation, and movement of bed materials.

Flow pattern near the suction

Brahme & Herbich (1986) investigated the flow field and sediment pickup near the inlet of the pipe. They performed a series of experiments to study the flow field for varying suction pipe diameter, suction inlet depth, and inlet discharge (Q). A negligible change in the velocity was seen when the pipe diameter was increased at a constant discharge. Velocity below the suction mouth was found relatively high but dropped rapidly with distance away from the suction mouth. They plotted a graph of the velocity variation in the vicinity of the suction inlet for $Q = 0.0032\ m^3/s$, $C = 10.16$ cm, and $D = 2.8$ cm, as shown in Figure 2. Here in the plot, Z is the distance along the center-line of the suction pipe, and $Z = 0$ is at the bed level. They found that the maximum velocity (0.1 m/s) at the suction inlet decreases to a minimum of 0.0098 m/s at a distance of 0.26 m away from centre-

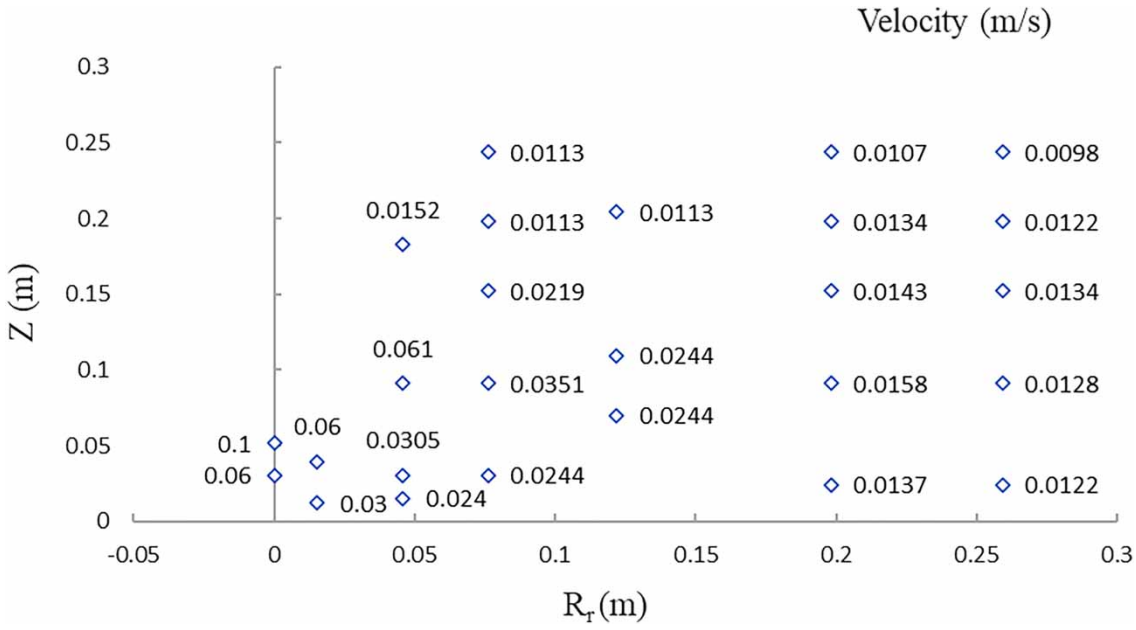

Figure 2 | Velocity variation near the suction inlet pipe for Q = 0.0032 m^3/s, C = 10.16 cm, and D = 2.8 cm. (Brahme & Herbich 1986).

line of the suction pipe. They observed that the velocity decrease as we move away from the suction inlet (vertically or horizontally).

Sediment movement

Dey *et al.* (2020) stated that during fluid flow over the sediment, bed materials are acted upon with a hydrodynamic force which combines shear stress (τ_o) at the particle surface and pressure intensity difference (ΔP) acting normal to it. The hydrodynamic force resolved into two components, lift force ($\vec{F}^l$) acting in the flow direction and drag force ($\vec{F}^s$) acting normal to it, as in Figure 3.

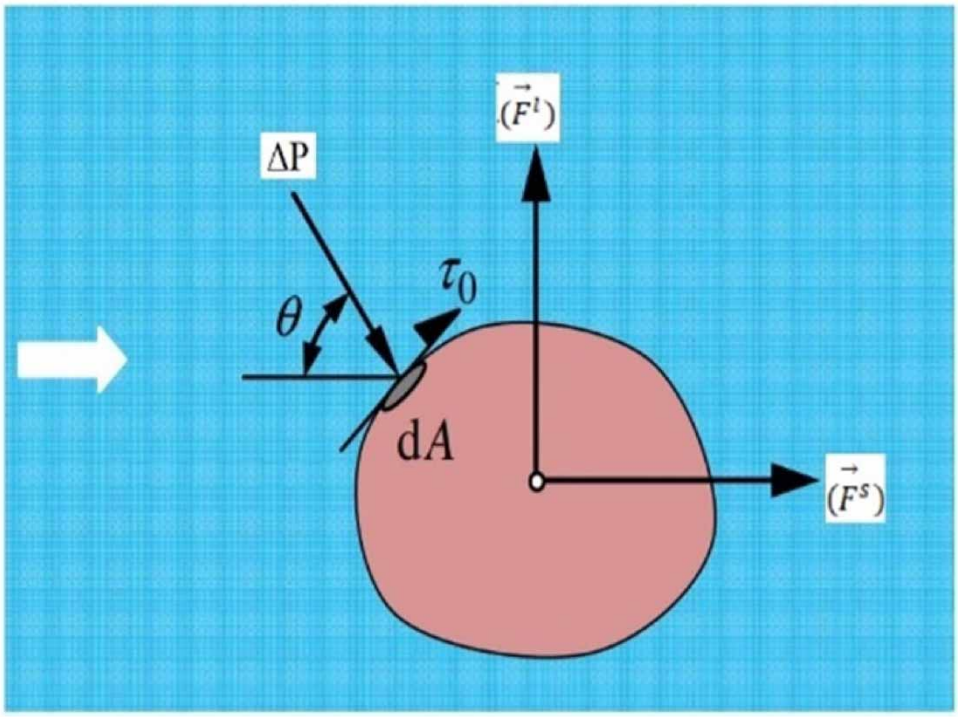

Figure 3 | Lift and drag forces on a particle placed in a fluid flow (Dey *et al.*, 2020).

The pore pressure gradient generated due to flow represents a hydraulic force at the sediment grains (Rehbinder 1976). This hydraulic force is similar to Archimedes' lift force for porosity lesser than unity. The shear stress represents the drag force acting at the sediment grains. The shear force is proportional to the cross-sectional area of grains (A). The removal takes place only when lift force ($\vec{F}^l$) dominates over shear force ($\vec{F}^s$). The ratio of these two forces provides conditions for bed material movement during hydro-suction as given below in Equation (1) (Rehbinder 1994).

$$\frac{\vec{F}^l}{\vec{F}^s} = \frac{\sqrt{\pi}}{C_2}\frac{\partial P}{\partial \zeta}\frac{1}{\xi}A\left(\frac{d_{50}}{C_0}\right)^{1/2}\left(\frac{Q}{C_0^2 v}\right)^{1/2} \tag{1}$$

Here $\xi = 0.5D/C_o$ and $\zeta = C/C_o$, C_0 is initial suction inlet depth, ϑ is kinematic viscosity, $\partial P/\partial\zeta$ is pore pressure gradient, C_2 is a constant, and Q is an inlet discharge. The initiation of bed materials movement occurs only after the suction inlet is below the critical inlet depth (C_{cr}). Just below the pipe, at $\xi = 0$, $1/\xi$ tends to infinity, indicating no sediment movement. These forces vanish for distances far away from the siphon inlet, so the equation becomes irrelevant for such a case. At the initiation, a crater is formed near the periphery of the pipe and gets deposited at the center. This suggests that the bed particles are dragged into the scour hole, guiding the hole size grow in the radial direction, as shown in Figure 4(a). As this deposition grew, the flow field changed, causing the removal of the entire interface, and an equilibrium is achieved, as shown in Figure 4(b).

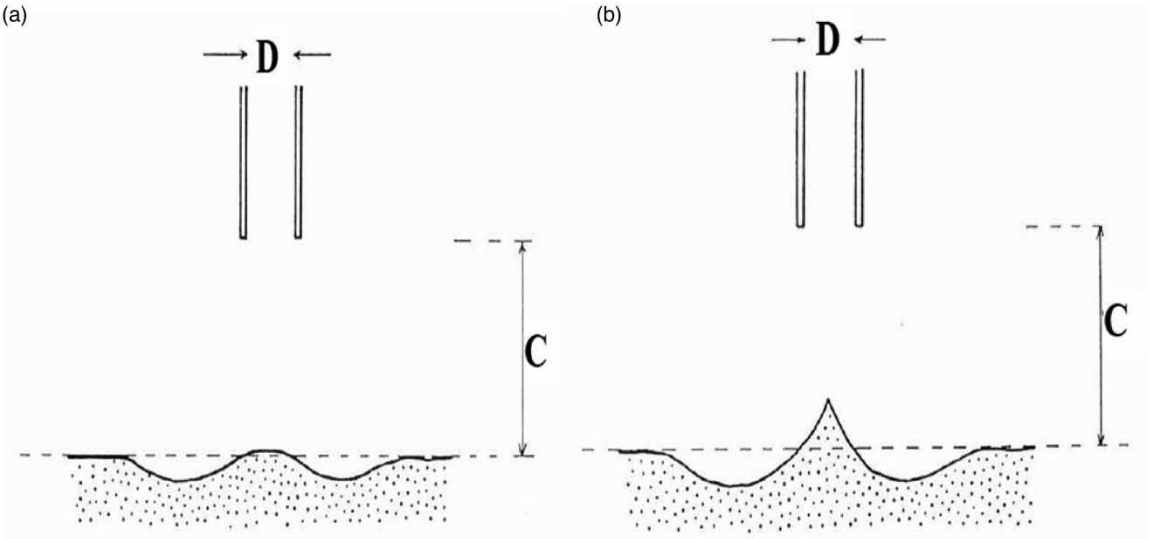

Figure 4 | Sketch of crater (a) at the initiation of flow; (b) at the equilibrium (Rehbinder 1994).

Hotchkiss & Huang (1995) studied hydraulic principles and design procedures of a hydro-suction sediment removal system (H.S.R.S.) and found that maximum sediment suction occurs when sediment particles verge deposition near the pipe. This maximum deposition is referred to as being between a heterogeneous flow regime and a flow regime with a moving bed.

Asiaban *et al.* (2017) investigated hydro-suction performance to remove cohesive sediment in low head reservoirs. They found that the scour hole reaches its maximum depth during the initial stage of hydro-suction; afterward, the peripheral sediment is dragged in from the sidewall towards the center. They reported that the conical heap at the center is absent in some cases, indicating the presence of vortices beneath the siphon inlet. The absence of a conical heap at the center for C = 2.5 cm is shown in Figure 5. They found that cohesive sediments have more resistance to sediment movement than non-cohesive sediments. As the cohesive property of sediment prevents the failure of the scour hole, it will be more difficult for the sediment to move during hydro-suction.

Brahme & Herbich (1986) found that sediment resuspension created by flow rotation near the suction inlet and lift generated through suction plays a significant role in sediment movement. The velocity just below the pipe was found maximum and decreased away from the inlet. Thus, after the initial sediment removal, any further removal is of the sediment in suspension.

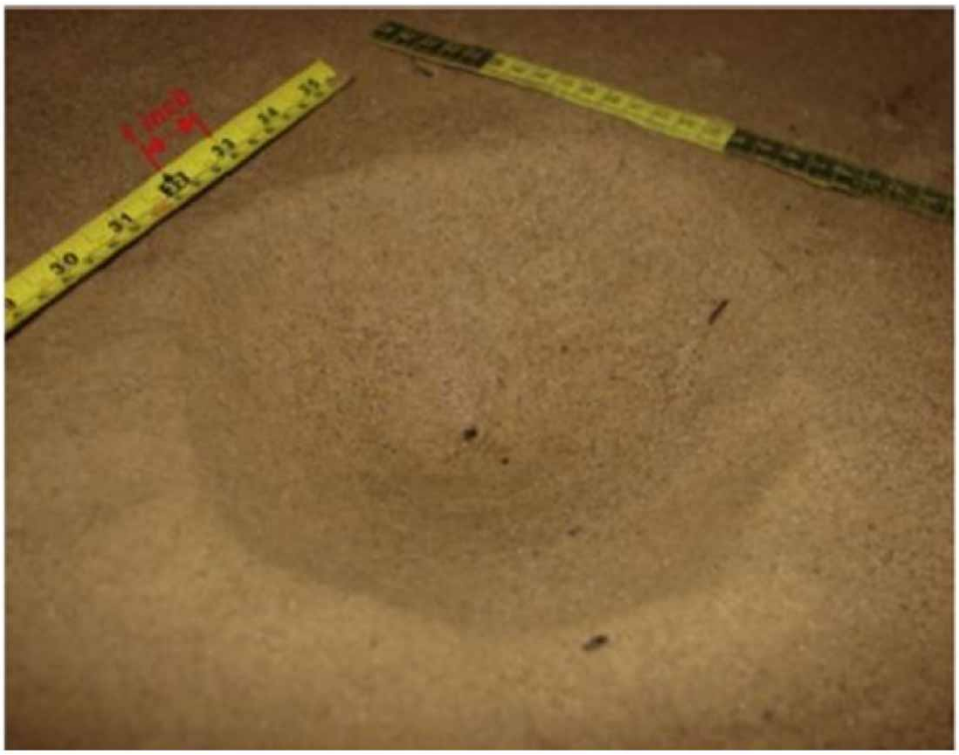

Figure 5 | Scour hole formed in fine sediment for C = 2.5 cm. (Asiaban *et al.* 2017).

Pu Yang *et al.* (2020) studied sediment scour caused by a vertical suction pipe and found that the suction inflow lifts off only the materials below the suction inlet. The peripheral materials were hydraulically dragged to the center, a part of which was removed with fluid flow, and the rest were deposited below the inlet, forming a hump. A diagrammatic sketch of sediment movement by hydro-suction is shown in Figure 6.

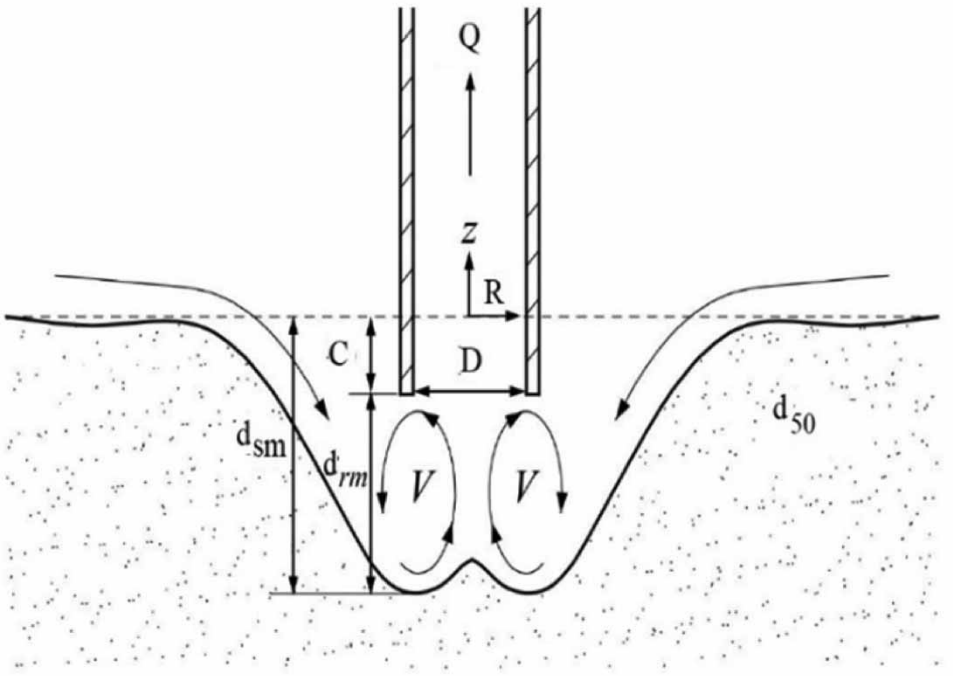

Figure 6 | Diagrammatic sketch of sediment movement by hydro-suction (Yang *et al.* 2020).

Scour profile

Ullah *et al.* (2005) investigated scouring created by a suction flow through suction inlet set vertically, above/on/below the surface of a cohesionless sand bed. The main interests of their investigation were to get maximum scour depth, the maximum radius of the scour hole, and scour hole profile. They performed a series of experiments with a suction pipe of D = 9.7 mm, 20.4 mm, and 13.9 mm, C ranging from −101.6 mm to 6.4 mm, and V_i ranging from 0.34 to 6.41 m/s. They found that the scour profiles are analogous for suction inlet depth; at or above the bed surface. The scour profile below the suction inlet for $C < 0$ is similar to the case when $C \geq 0$, and the rest of the profile follows linear variation up to the sediment surface. They plotted scour profiles at equilibrium for C = −25.4 mm and −38.1 mm, V_i ranging from 0.99 m/s to 2.42 m/s with a constant D = 13.9 mm, as shown in Figure 7.

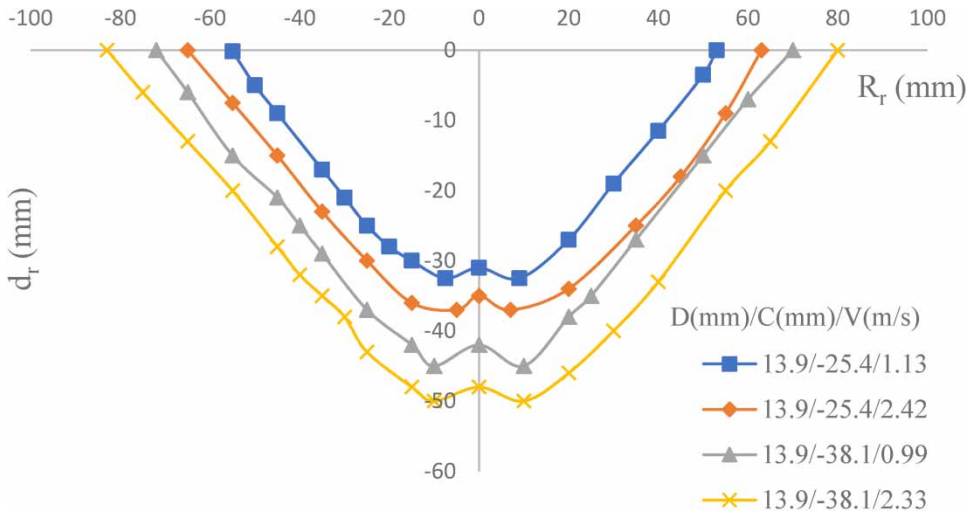

Figure 7 | Experimental scour profile at equilibrium (Ullah *et al.* 2005).

They found that d_{sm} and R_s decrease with a decrease in inlet velocity for the same D and C, as can be seen from Figure 7. They found that the scour profile follows the movement of bed material during hydro-suction, thus forming a semi-circular profile with a hump at the center.

Su Chin *et al.* (2010) studied pressure and velocity distribution and sediment removal efficiency of a siphon. They performed experiments for C = 13, 26 and 52 mm, Q ranging from 0.32×10^{-3} to 5.9×10^{-3} m^3/s. They plotted scour depth at different scour radii for three values of C, as shown in Figure 8, and found a similar scour profile as obtained by Ullah *et al.* (2005). They also found that as the C increases, the scour depth also decreases. A hump was seen below the suction inlet, and maximum scour depth was formed at some distance from the center.

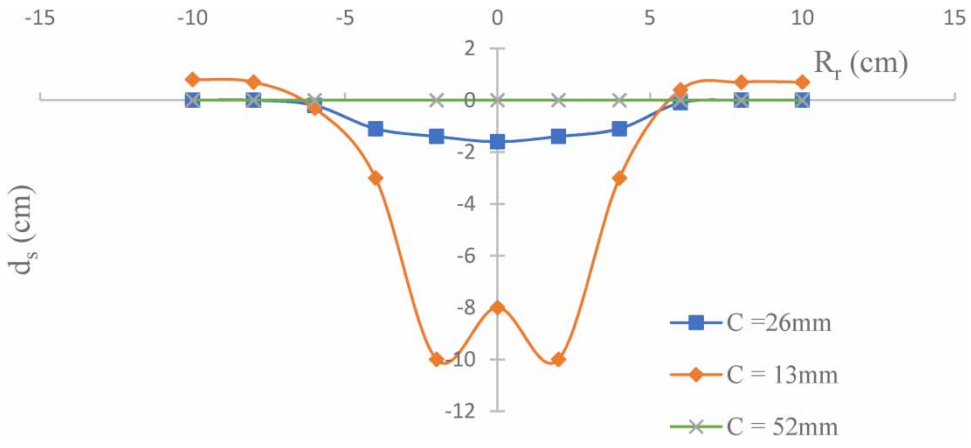

Figure 8 | A plot of scour profile (Su Chin *et al.* 2010).

Ke *et al.* (2016) investigated how the degree of consolidation affects hydro suction performance. They performed experiments for consolidation duration (t_c) = 7 days, C = −8 cm, D = 1.3 cm, and Q = 157 × 10^{-6} m^3/s and plotted the scour profile evolution at 30 s intervals in cohesive sediment, as shown in Figure 9. The origin of the coordinate system was placed at the center-line of the suction pipe. They observed that at the initiation of hydro-suction, sediment in the periphery of the pipe is sucked in, forming a crater with steep inward-facing slopes and having its apex at the suction inlet.

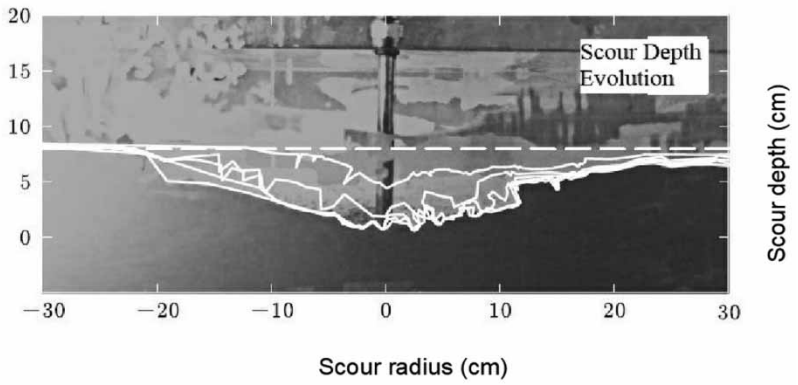

Figure 9 | Scour profile evolution plotted at 30 s intervals in cohesive sediment for t_c = 7days, C = −8 cm, D = 1.3 cm, and Q = 157 × 10^{-6} m^3/s (Ke *et al.* 2016).

Elgamal & Fouli (2020) investigated sediment removal through a siphon action using a dual suction pipe. In the experimental setup, they took only half a section, considering the other section as symmetry. They performed a series of experiments on poorly graded sand having d_{50} = 1 mm, suction pipes of D = 6 mm, 9.5 mm, and 13.8 mm, C ranging from 0 to 7 mm, and V_i ranging from 4 to 4.9 m/s. They observed that the hump at the center of the scour holes did not appear in their experiment. They stated that one possible reason that a hump was not observed is the effect of the tank front glass wall in breaking vortex actions around the siphon pipe inlet.

Removal equations

A few equations governing hydro-suction are also found in the literature. Brahme & Herbich (1986) studied the hydraulic model for the design of hydro-suction. They studied the flow field and sediment pickup at the suction inlet. They studied hydro-suction studies varying D, C, Q, and the different bed materials: microbeads, fine sand, medium sand, and coal. Their purpose was to determine the similitude criteria for sediment pickup behavior at the suction cutter-head intake. They plotted a graph between (C/D) and $(QC/R_s^2\vartheta 10^{-3})$ for all sediment, a straight-line relationship between the two parameters. They plotted normalized data using fine sand as a basis (specific gravity = 2.66 and d_{fs} = 0.25 mm), as shown in Figure 10.

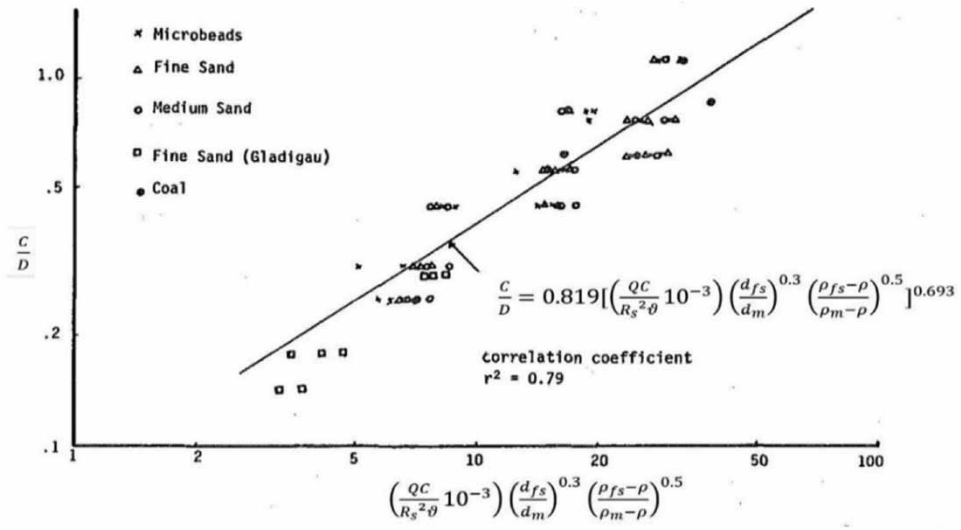

Figure 10 | A plot of C/D v/s normalized $QC/R_s^2\vartheta 10^{-3}$ for all the sediment (Brahme & Herbich 1986).

The best fit line for the graph having a correlation coefficient of 0.79 is shown in Equation (2).

$$\frac{C}{D} = 0.819\left\{\left[\frac{QC}{R_s^2\vartheta}10^{-3}\right]\left[\frac{d_{fs}}{d_m}\right]^{0.3}\left[\frac{\rho_{fs}-\rho}{d_m-\rho}\right]^{0.5}\right\}^{0.693} \tag{2}$$

Here, ρ is density of water, ρ_{fs} is density of fine sand, and ρ_m is density of material under consideration, d_{fs} is particle diameter of fine sand, and d_m is particle diameter of material under consideration.

Ullah *et al.* (2005) studied scouring through a suction pipe placed vertically above, on, and below the surface of a cohesionless sand bed. They performed a series of experiments varying C, V_i, and D. Using the experimental results, they proposed equations for predicting scour profile, as given below in Equations (3) and (4).

$$\frac{d_r}{d_{sm}} = -1.12\left(\frac{R_r}{R_t}\right)^3 + 3.6\left(\frac{R_r}{R_t}\right)^2 - 1.71\left(\frac{R_r}{R_t}\right) - 0.78 \quad \left(0 < \frac{R_r}{R_t} \le 1.2\right) \tag{3}$$

$$\frac{d_r}{d_{sm}} = -2.12\frac{R_r}{R_t} - 2.11 \quad \left(\frac{R_r}{R_t} > 1.2\right) \tag{4}$$

Here, d_{sm} is defined by Equation (5), R_t is scour radius at the inlet level defined by Equation (6), F_o is densimetric Froud number defined by Equation (7).

$$\frac{d_{sm}}{D} = 0.17F_0^{0.5} \tag{5}$$

$$\frac{R_t}{D} = 0.64F_0^{0.41} \tag{6}$$

$$F_0 = \frac{V_i}{\sqrt{gD\frac{\rho_s-\rho}{\rho}}} \tag{7}$$

An equation for critical suction inlet depth was also provided, as in Equation (8) below

$$\frac{C_{cr}}{D} = 0.25F_0^{0.43} \tag{8}$$

Sadatomi *et al.* (2015) studied the self-designed siphonic sediment removal system using suction pipe of varying D and sediment of varying d_{50}. They took non-spherical sediment with $d_{50} = 1.4$ mm and 3.4 mm and round-edged siphon inlet with D = 30 and 40 mm for study. They compared the results with their earlier study (Tajima 2010) where they took spherical sediment with $d_{50} = 1.2$ mm, 2.1 mm, and 4.0 mm, and square-edged siphon inlet with D = 20 and 30 mm. Tajima (2010) defined particle volume flow rate fraction (βs) as a ratio of particle volume flow rate and the summation of water volume flow rate and particle volume flow rate. They proposed an equation to predict βs, as given in Equation (9) below.

$$\beta_s = 0.7233(e)^{-5.27(d_{50}\backslash D)}(G_s)^{-0.03}\left(\frac{d_{50}U_p}{\vartheta}\right)^{-0.02} \tag{9}$$

Here, U_p is the settling velocity of the single particle in stagnant water, and G_s is a specific gravity of sediment.

Sadatomi *et al.* (2015) proposed a modified relation including the effect of horizontal siphon length (L), as given in Equation (10). $L_{H.}$ is the length of the horizontal siphon pipe connecting the up-rising siphon pipe and the down-coming siphon pipe, as shown in Figure 11.

$$\beta_s = K\left[\left(\frac{d_{50}}{D}\right)^{-0.2}\left(\frac{L_H}{D}\right)^{-0.07}\left(\frac{d_{50}U_p}{\vartheta}\right)^{-0.2}\right] \tag{10}$$

Here, K = 1.09 and 0.86 for a spherical and non-spherical particle in a square siphon inlet, respectively, and 1.17 and 0.085 for a spherical and non-spherical particle in a rounded siphon inlet, respectively.

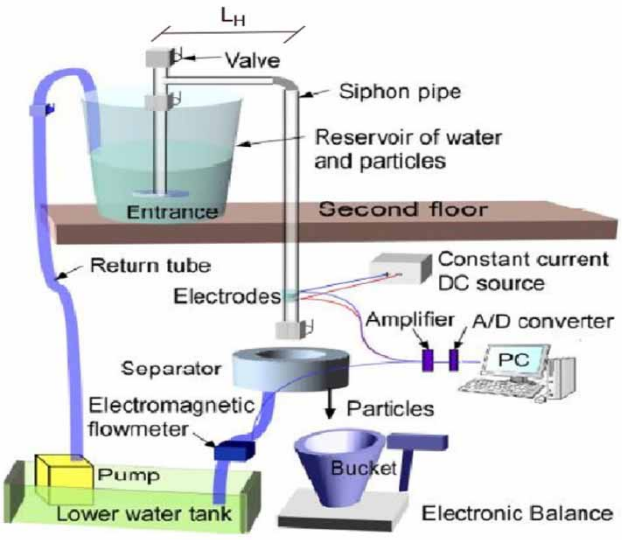

Figure 11 | Experimental setup of Sadatomi *et al.* (2015).

Wun Tao ke *et al.* (2016) investigated the effects of the degree of consolidation of sediments on hydro suction performance. They performed experiments using suction pipe of D = 1.3 cm and 8.0 cm, Q ranging from 0.54×10^{-4} to 1.77×10^{-4} m^3/s, sediment of $d_{50} = 0.0079$ mm, and degrees of consolidation achieved after consolidation times (t_c) = 1, 5, and 7 days, 2 weeks, and 3 months. They provided an equation predicting critical suction inlet depth, as given below in Equation (11).

$$C_{cr} = \left[\frac{Q^2}{(4/5)^5 2\pi^2 \frac{(\rho_s - \rho)g}{\rho_s}} \right]^{1/5} \tag{11}$$

Pu Yang *et al.* (2020) studied hydro-suction removal of sediment, focusing on equilibrium scour depth in the vertical direction. The analysis started with Shields' theory of incipient motion at critical inlet depth as

$$(\tau_0)_{cr} \sim (\rho_s - \rho)\, g d_{50} (\tau_*)_{cr} \tag{12}$$

Here, τ_o is shear stress and τ_* is Shield's dimensionless parameter.

The shear stress obtained from the momentum transfer hypothesis can be written as according to Equation (13)

$$\tau_0 \sim \rho v_n v_t \tag{13}$$

Here v_n *and* v_t are fluctuating velocities perpendicular and parallel to the interface.

Using the above background, they proposed the relation between equilibrium maximum scour during hydro-suction with densimetric Froud number, as given below in Equation (14).

$$F_0 \sim \left(\frac{D}{d_{sm}} \right)^{-1/6} \tag{14}$$

Temporal sediment concentration

Most of the sediment is removed during the initial stage of hydro-suction, depending on the height of the suction inlet. Afterward, any further removal is due to the change in the flow field within the scour hole. Ullah *et al.* (2005) found that the deeper suction pipe placed in the sediment bed has a more extended initial period of high sediment removal rate. They also observed that most sediments are removed within a minute of the scouring process. After which, removal was only when there was a change in the flow pattern.

Wun-Tao Ke *et al.* (2016) studied sediment concentration in the pipe in their investigation using the Anton-Paar oscillating U-tube device. They found that maximum sediment removal took place within a few seconds of hydro-suction; after that, the sediment removal is nearly negligible. They observed a secondary peak after a few minutes of the first peak, produced mainly by the failure of the side slope of the scour hole and being sucked in through hydro-suction.

Asiaban *et al.* (2017) observed a steep decrease in the sediment concentration within the first few seconds, and it became approximately negligible after that. They plotted a graph showing the variation of sediment concentration in a pipe with time, as shown in Figure 12.

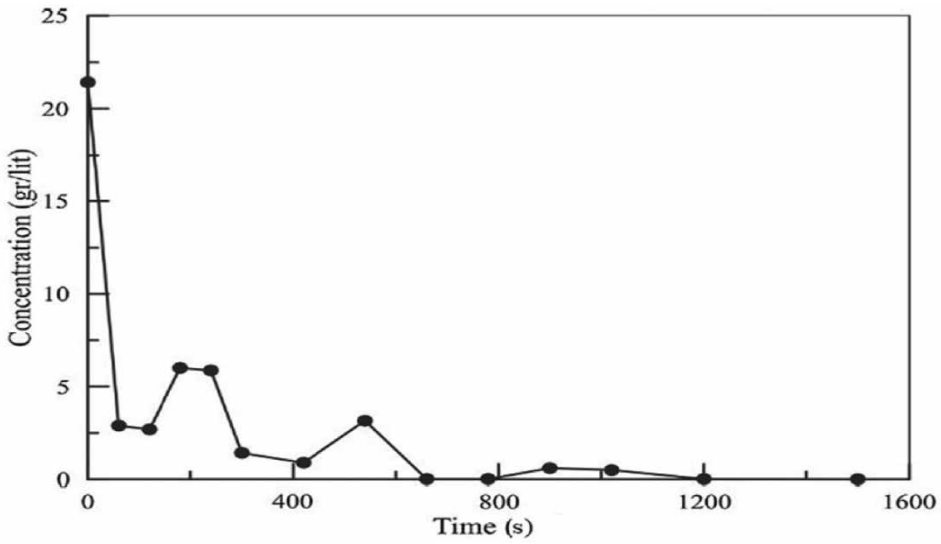

Figure 12 | Temporal variation of sediment concentration (Asiaban *et al.* 2017).

This plot shows that most of the removal takes place within the first few seconds of initiation of suction, forming the deepest scour hole. Any further sediment withdrawal is due to the sliding of materials from the side slope of scour hole and collapsing within the hole, causing change in the flow field.

CONCLUSIONS

Review of the literature indicates that hydro-suction is a function of the median size of sediment, the suction pipe's diameter, height of suction inlet, and inlet velocity. Bed material movement, temporal variation of sediment concentration in the pipe, scour profile during hydro-suction have been investigated by the various investigators. It is found that there is no scouring until the suction inlet pipe is set below the critical inlet depth. As C decreases below the C_{cr}, movement of bed material initiates. The closer the value of C to zero, the more will be the removal of bed material. At the initiation of hydro-suction, initial scouring is due to lift regulated by inlet velocity forming a scour hole with the deepest scour hole. The sediment from the periphery of the suction pipe roll toward the center of scour hole. Most of these are sucked in, and some get deposited, forming a hump at the center. Any further removal after this is due to the sliding of unstable materials from the side slope of scour hole and collapsing within it, causing change in the flow field. This phase does not last long and mainly depends upon the value of C. After this phase, an equilibrium state is reached, causing no further movement of bed material. It is noted that scour hole profiles for $C > 0$ and $C = 0$ are similar in appearance. For $C < 0$, the scour profile around the suction inlet is identical to that of the case when $C \geq 0$, but the rest of the profile follows the linear variation up to the sediment surface. Sediment concentration in the suction pipe is maximum for the first few seconds; then, a sudden drop in the sediment concentration is observed. A second peak in the sediment concentration is seen, marking the change in flow pattern due to failure of the sidewall materials and being sucked in through hydro-suction. Relationships predicting equilibrium maximum scour depth and critical suction inlet depth during hydro-suction are also provided that can be used to predict these values knowing the required variable.

DATA AVAILABILITY STATEMENT

All relevant data are included in the paper or its Supplementary Information.

REFERENCES

Asiaban, P., Kouchakzadeh, S. & Asiaban, S. 2017 Enhanced hydro-suction performance for cohesive sediment removal in low-head reservoirs. *Ain Shams Engineering Journal* **8**(4), 491–497.

Azamathulla, H. M. 2014 Development of GEP-based functional relationship for sediment transport in tropical rivers. *Neural Computing and Applications* **24**(2), 271–276.

Azamathulla, H. M., Cuan, Y. C., Ghani, A. A. & Chang, C. K. 2013 Suspended sediment load prediction of river systems: GEP approach. *Arabian Journal of Geosciences* **6**(9), 3469–3480.

Brahme, S. B. & Herbich, J. B. 1986 Hydraulic model studies for suction cutterheads. *Journal of Waterway, Port, Coastal, and Ocean Engineering* **112**(5), 591–606.

Dey, S., Ali, S. Z. & Padhi, E. 2020 Hydrodynamic lift on sediment particles at entrainment: present status and its prospect. *Journal of Hydraulic Engineering* **146**(6), 03120001.

Elgamal, M. & Fouli, H. 2020 Sediment removal from dam reservoirs using syphon suction action. *Arabian Journal of Geosciences* **13**(18), 1–10.

Hotchkiss, R. H. & Huang, X. 1995 Hydrosuction sediment-removal systems (H.S.R.S.): principles and field test. *Journal of Hydraulic Engineering* **121**(6), 479–489.

Ke, W. T., Chen, Y. W., Hsu, H. C., Toigo, K., Weng, W. C. & Capart, H. 2016 Influence of sediment consolidation on hydrosuction performance. *Journal of Hydraulic Engineering* **142**(10), 04016037.

Obialor, C. A., Okeke, O. C., Onunkwo, A. A., Fagorite, V. I. & Ehujuo, N. N. 2019 *Reservoir Sedimentation: Causes, Effects, And Mitigation*.

Patra, B., Gir, S. & Narayan, P. 2019 Reservoir Sedimentation in Indian Dams: Trends and Challenges. In *International Dam Safety Conference*, Bhubaneswar, India.

Pishgar, R., Ayyoubzadeh, S. A., Ghodsian, M. & Saneie, M. 2018 The influence of burrowing-type suction pipe geometrical and mechanical specifications on the hydro-suction method performance. *ISH Journal of Hydraulic Engineering* **27**(6), 1–10.

Rehbinder, G. 1976 Some aspects on the mechanism of erosion of rock with a high speed water jet. In *Proc. of the 3rd International Symp. on Jet Cutting Technique*, Chicago.

Rehbinder, G. 1994 Sediment removal with a siphon at critical flux. *Journal of Hydraulic Research* **32**(6), 845–860.

Sadatomi, M., Nagano, T. & Kawahara, A. 2015 Siphonic removal of sediments in water reservoirs–Additional experiment for model revision. *International Journal of Environmental Science and Development* **6**(6), 409.

Shrestha, H. S. 2012 Application of hydrosuction sediment removal system (H.S.R.S.) on peaking ponds. *Hydro Nepal: Journal of Water, Energy and Environment* **11**, 43–48.

Su-Chin, C. H. E. N., Shun-Chang, W. A. N. G. & Chun-Hung, W. U. 2010 Sediment removal efficiency of siphon dredging with wedge-type suction head and float tank. *International Journal of Sediment Research* **25**(2), 149–160.

Tajari, M., Dehghani, A. A., Meftah Halaghi, M. & Azamathulla, H. 2020 Use of bottom slots and submerged vanes for controlling sediment upstream of duckbill weirs. *Water Supply* **20**(8), 3393–3403.

Tajima, N. 2010 Dredging of sediment in dam utilizing siphonage with sliding outer tube. *Japanese Journal of Multiphase Flow* **24**(1), 70–76.

Tong, J., Yasufuku, N., Omine, K. & Kobayashi, T. 2010 Experimental study on the dewatering behavior of the dredged mud with horizontal drainage by siphon method. *Geosynthetics Engineering Journal* **25**, 267–270.

Ullah, S. M., Mazurek, K. A., Rajaratnam, N. & Reitsma, S. 2005 Siphon removal of cohesionless materials. *Journal of Waterway, Port, Coastal, and Ocean Engineering* **131**(3), 115–122.

Yang, P., Wang, G. & Zhong, L. 2020 Suction removal of cohesionless sediment. *Energies* **13**(20), 5436.

Zakaria, N. A., Azamathulla, H. M., Chang, C. K. & Ghani, A. A. 2010 Gene expression programming for total bed material load estimation – a case study. *Science of the Total Environment* **408**(21), 5078–5085.

Zhou, Y., Zhang, Y., Tang, P., Chen, Y. & Zhu, D. Z. 2013 Experimental study of the performance of a siphon sediment cleansing set in a C.S.O. chamber. *Water Science and Technology* **68**(1), 184–191.

Zulkefli, Z. F., Zainol, M. R. R. M. A., Abas, M. A. & Abustan, I. 2019. A review: A removal sediment by using siphon technique in water reservoir. In A.I.P. Conference Proceedings (Vol. 2129, No. 1, p. 020084) (S. Z. Bin Abd. Rahim & Mohd M. Al-Bakri Bin Abdullah, eds). A.I.P. Publishing L.L.C, Jawa Barat, Indonesia.

First received 5 February 2022; accepted in revised form 27 May 2022. Available online 7 June 2022